

SANDIA REPORT

SAND97-2328 • UC-401

Unlimited Release

Printed October 1997

Report of Work Done for Technical Assistance Agreement 1269 Between Sandia National Laboratories and the Watkins-Johnson Company: “Chemical Reaction Mechanisms for Computational Models of SiO₂ CVD”

Pauline Ho, Justine Johannes, Vladimir Kudriavtsev

Prepared by
Sandia National Laboratories
Albuquerque, New Mexico 87185 and Livermore, California 94550

Sandia is a multiprogram laboratory operated by Sandia Corporation, a Lockheed Martin Company, for the United States Department of Energy under Contract DE-AC04-94AL85000.

Approved for public release; further dissemination unlimited.



Sandia National Laboratories

Issued by Sandia National Laboratories, operated for the United States Department of Energy by Sandia Corporation.

NOTICE: This report was prepared as an account of work sponsored by an agency of the United States Government. Neither the United States Government nor any agency thereof, nor any of their employees, nor any of their contractors, subcontractors, or their employees, makes any warranty, express or implied, or assumes any legal liability or responsibility for the accuracy, completeness, or usefulness of any information, apparatus, product, or process disclosed, or represents that its use would not infringe privately owned rights. Reference herein to any specific commercial product, process, or service by trade name, trademark, manufacturer, or otherwise, does not necessarily constitute or imply its endorsement, recommendation, or favoring by the United States Government, any agency thereof or any of their contractors or subcontractors. The views and opinions expressed herein do not necessarily state or reflect those of the United States Government, any agency thereof or any of their contractors.

Printed in the United States of America. This report has been reproduced directly from the best available copy.

Available to DOE and DOE contractors from
Office of Scientific and Technical Information
PO Box 62
Oak Ridge, TN 37831

Prices available from (615) 576-8401, FTS 626-8401

Available to the public from
National Technical Information Service
US Department of Commerce
5285 Port Royal Rd
Springfield, VA 22161

NTIS price codes
Printed copy: A08
Microfiche copy: A01

SAND97-2328
Unlimited Release
Printed October 1997

**Report of Work done for Technical Assistance Agreement 1269 between Sandia National
Laboratories and the Watkins-Johnson Company:
“Chemical Reaction Mechanisms for Computational Models of SiO₂ CVD”**

Pauline Ho

Chemical Processing Science Department

Justine Johannes

Plasma and Aerosol Sciences Department

Sandia National Laboratories

P.O. Box 5800

Albuquerque, NM 87185-0601

Vladimir Kudriavtsev

Watkins-Johnson Company

Scotts Valley, CA 95066

Abstract

Previous work done at Sandia on reaction mechanisms for the chemical vapor deposition (CVD) of silicon oxide from tetraethoxysilane (TEOS) and ozone is documented and tested in computational models at Watkins-Johnson. Recommendations for future work in this area are discussed.

Report of Work done for Technical Assistance Agreement 1269 between Sandia National Laboratories and the Watkins-Johnson Company:

“Chemical Reaction Mechanisms for Computational Models of SiO₂ CVD”

I. Introduction

The use of computational modeling to improve equipment and process designs for chemical vapor deposition (CVD) reactors is becoming increasingly common. Commercial codes are available that facilitate the modeling of chemically-reacting flows, but chemical reaction mechanisms must be separately developed for each system of interest.

One of the products of the Watkins-Johnson Company (WJ) is a reactor marketed to semiconductor manufacturers for the atmospheric-pressure chemical vapor deposition (APCVD) of silicon oxide films. In this process, TEOS (tetraethoxysilane, Si(OC₂H₅)₄) and ozone (O₃) are injected (in nitrogen and oxygen carrier gases) over hot silicon wafers that are being carried through the system on a moving belt. As part of their equipment improvement process, WJ is developing computational models of this tool. In this effort, they are collaborating with Sandia National Laboratories (SNL) to draw on Sandia’s experience base in understanding and modeling the chemistry of CVD processes.

Although the TEOS/O₃ system has been the subject of much work,¹ including previous work at WJ,^{2,3} we do not include a review of the literature here. An initial collaborative project by Justine Johannes (SNL) and Simin Moktari (WJ) was done in 1995 under the auspices of the EDSC (Equipment Design Service Center) at SNL. The purpose of the EDSC was to facilitate small projects between SNL researchers and industrial partners, and was part of a large CRADA (cooperative research and development agreement) between SNL and SEMATECH. The present small technical assistance agreement by Pauline Ho (SNL) and Vladimir Kudriavtsev (WJ) represents a follow-on to the previous work and has two objectives. First is to document the mechanism developed in the previous work and implement it into the computational models now being developed at WJ to test its performance. Second is to gather other existing chemical

knowledge relevant to the TEOS/O₃ system and to develop recommendations for improved chemical reaction mechanisms.

II. Development of 1995 mechanism

There are a wide variety of reactions that are likely to occur in the TEOS/O₃ system (to be discussed in more detail in Section IV below). The most important classes of reactions are 1) ozone decomposition to form O atoms and other reactions that interconvert O₃, O and O₂, 2) TEOS reactions with O atoms and/or ozone to form gas-phase intermediate species, 3) reaction of various gas-phase species with the surface, and 4) interconversion of surface species involving the generation of gaseous byproducts. Of course, an intermediate species produced in any given gas-phase reaction can further decompose and/or react with any other gas-phase species, possibly forming a radical chain. However, the reaction mechanism developed in 1995 was intended to be transferred to simulations being done at WJ. At that time, the codes in use could handle only 10 reacting chemical species, which made it impossible to include a reasonable number of elementary chemical reactions. This constraint, combined with limited resources, led to the development of a mechanism using “overall” or “lumped” reactions that were fit to experimental deposition-rate data.

The mechanism was developed using a code, SPIN,⁴ based on CHEMKIN⁵ and Surface-CHEMKIN.⁶ These modular software packages allow chemical reactions to be described in a simple but flexible, user-friendly manner. Detailed descriptions of these codes and the formats of the input files are available elsewhere,^{5,6} so only a brief description is included here. The basic structure consists of standard equations representing reversible and/or irreversible chemical reactions with accompanying rate parameters of the form $k = A T^\beta \exp(-E_a/RT)$, (the three parameters given on the same line as the reaction are A, β , and E_a). For the reaction of a gas-phase species with the surface, the rate parameter can also be specified as a sticking coefficient. Thermochemical data are needed to calculate rates for reverse reactions from the forward reaction rates and are in the form of seven-parameter polynomial coefficients for $C_p(T)$, $H(T)$ and $S(T)$. These data may either be included in the input file, or obtained by the code from a database. For surface species, dummy data are often supplied to satisfy error-checking routines

in the software, even though the reactions are irreversible so that the data are not actually used. Although a variety of units can be specified, the defaults are moles, cm and s.

Tables 1 and 2 give the 1995 mechanism for TEOS/O₃ CVD in the form of input files for CHEMKIN and Surface-CHEMKIN. In this mechanism, the following reactions directly lead to the deposition. Gas phase reaction 1: the gas-phase decomposition of O₃ to O atoms. Gas phase reaction 4: the reaction between O atom and TEOS forming a more-reactive intermediate species (designated here as Si(OC₂H₅)₃OH, triethoxysilanol, although it's probably something different in reality). Surface reaction 1: the reaction of the gas-phase intermediate species with the surface. Surface reactions 3 and 4: regeneration of the reactive surface species by desorption of "blocking groups".

The other reactions in the mechanism serve other purposes. In the gas phase, reaction 2, the reaction of two ozone molecules to form three oxygen molecules, provides an alternate ozone loss pathway. Gas phase reaction 3 is actually a subset of the first reaction and, as written, is so slow that it could be eliminated. Gas phase reaction 4, the reaction of TEOS with ozone, is included for completeness, although the estimated rate constant is quite low. The last gas phase reaction represents the loss of the reactive intermediate via formation of a gaseous byproduct that does not lead to film deposition, and thus the reaction has been made irreversible. This second "intermediate" species has been designated as O=Si(OC₂H₅)₂, diethoxysilane, although this is again a "placeholder" for what is probably a variety of molecules. On the surface, the reaction of TEOS with the surface is included for completeness; experiments have shown that TEOS (in the

Table 1. CHEMKIN input file for gas-phase chemistry in 1995 mechanism			
ELEMENTS H C O N			
SI			
END			
SPECIES			
O O2 O3 CH3HCO SI(OC2H5)4 OSI(OC2H5)2			
SI(OC2H5)3OH H2O N2 C2H4 CH3CH2OH			
END			
THERMO			
REACTIONS			
O3+M=O2+O+M	1.00e+13	0.00	18000! Comb. Book 1980
2O3=3O2	5.00e+13	0.00	22000! Ho from Kond.
O3+O2=O+2O2	2.9e+6	0.00	23340! Kondratiev
SI(OC2H5)4+O = SI(OC2H5)3OH+CH3HCO	5.0e+16	0.00	5000!est. dHf and Kawa.
SI(OC2H5)4+O3 = SI(OC2H5)3OH+CH3HCO+O2	4.e+12	0.00	5000!guess
SI(OC2H5)3OH+M => OSI(OC2H5)2+CH3CH2OH+M	0.4e13	0.00	20000!Gill/Kim
END			

Table 2. CHEMKIN input file for surface chemistry in 1995 mechanism

```

MATERIAL/TEST1/
SITE/SIO2/      SDEN/1.1683E-9/
  SI(OH)(S)/1/ SI(OC2H5)3(S)/1/ SI(OC2H5)2OH(S)/1/
END
BULK SIO2(D)/2.33/
END
THERMO
  300.      600.      1685.
SI(OH)(S)   J 3/670   1H   1SI  10   0S   300.000  1685.000      1
  0.24753989E 01 0.88112187E-03-0.20939481E-06 0.42757187E-11 0.16006564E-13      2
-0.81255620E 03-0.12188747E 02 0.84197538E 00 0.83710416E-02-0.13077030E-04      3
  0.97593603E-08-0.27279380E-11-0.52486288E 03-0.45272678E 01      4
SI(OC2H5)2OH(S) J 3/670   3H  11SI  1C   4S   300.000  1685.000      1
  0.24753989E 01 0.88112187E-03-0.20939481E-06 0.42757187E-11 0.16006564E-13      2
-0.81255620E 03-0.12188747E 02 0.84197538E 00 0.83710416E-02-0.13077030E-04      3
  0.97593603E-08-0.27279380E-11-0.52486288E 03-0.45272678E 01      4
SI(OC2H5)3(S)   J 3/670   3H  15SI  1C   6S   300.000  1685.000      1
  0.24753989E 01 0.88112187E-03-0.20939481E-06 0.42757187E-11 0.16006564E-13      2
-0.81255620E 03-0.12188747E 02 0.84197538E 00 0.83710416E-02-0.13077030E-04      3
  0.97593603E-08-0.27279380E-11-0.52486288E 03-0.45272678E 01      4
SIO2(D)        J 3/67SI  10   100  000  0S   300.000  1685.000      1
  0.24753989E 01 0.88112187E-03-0.20939481E-06 0.42757187E-11 0.16006564E-13      2
-0.81255620E 03-0.12188747E 02 0.84197538E 00 0.83710416E-02-0.13077030E-04      3
  0.97593603E-08-0.27279380E-11-0.52486288E 03-0.45272678E 01      4
END

REACTIONS
SI(OC2H5)3OH+SI(OH)(S)=>SI(OC2H5)3(S)+H2O+SIO2(D)      0.05   0.00   0.0
STICK
SI(OC2H5)4+SI(OH)(S)=>SIO2(D)+SI(OC2H5)3(S)+H2O+C2H4      0.4e-7  0.00   0.00
STICK
SI(OC2H5)3(S)=>SI(OC2H5)2OH(S)+C2H4      8.55e12  0.00  25000.0
SI(OC2H5)2OH(S)=>SI(OH)(S)+CH3HCO+CH3CH2OH      2.85e12  0.00  25000.0
END

```

absence of O₃) has very low reactivity with an SiO₂ surface. The other two surface reactions eliminate carbon and hydrogen from the surface, while regenerating the surface silanol group that reacts with the gas-phase species.

The SPIN code, which simulates a one-dimensional stagnation flow, was used to do mechanism development and reaction-rate tuning. The reaction rates in the mechanism, especially for the gas-phase reactions, were initially set to values either taken from the literature or best estimates. Many of these rates were subsequently adjusted to get reasonable agreement with experimental data from WJ. As shown in Table 3, these simulations reproduced the deposition rates reasonably well, including the decrease in deposition rate with increasing temperature. Note that a variety of TEOS and O₃ flow rates were used. The mechanism was tuned to give deposition rates that were, in general, about 60% higher than the observed “belt deposition” experiments. However, these simulations underpredicted the deposition rates at the lowest temperatures.

Temperature (°C)	Total Flow (sccm)	TEOS Flow (sccm)	O ₃ /TEOS	O ₂ /TEOS	Experiment (Å/min)	SPIN (Å/min)
305	26000	25	6.5	165	4615	3235
365	22000	20	5	115	3796	2777
365	22000	30	5	115	4888	3967
365	22000	20	8	115	3781	2776
425	18000	25	3.5	165	2412	3321
425	18000	15	6.5	165	1621	3333
425	18000	25	9.5	165	1546	2000
425	18000	25	6.5	265	2129	3289
425	18000	25	6.5	165	2647	3307
485	16000	30	5	215	1706	2510
545	16000	25	6.5	165	1133	1557

III. Implementation of 1995 mechanism into two-dimensional reactor models

The mechanism developed in 1995 was not tested at the time in a full simulation of the WJ-1000 injector/reactor system, but only in the simplified description of the flow used in the SPIN code. Such a test became the first objective of the current project. Transferring the 1995 mechanism to the present code used at WJ, CFD-ACE,⁷ involved dealing with several issues.

The two software systems, CHEMKIN and CFD-ACE, use different sets of units, so conversion was needed. Pre-exponential factors in the CHEMKIN mechanism are written in terms of gram-moles, cm and s, with activation energies in cal/mole, whereas CFD-ACE uses pre-exponential factors in kgram-moles, m and s, with activation energies in Kelvins. Thus, a second order rate constant in the CHEMKIN input file of $1 \times 10^{13} \exp(-18000/RT) \text{ cm}^3/(\text{mole s})$ becomes $1 \times 10^{10} \exp(-9058/T) \text{ m}^3/(\text{kmole s})$ for CFD-ACE. Likewise, a third-order rate constant in CHEMKIN of $2 \times 10^{11} \exp(+6467/RT) \text{ cm}^6/(\text{mole}^2 \text{ s})$ becomes $2 \times 10^5 \exp(+3255/T) \text{ m}^6/(\text{kmole}^2 \text{ s})$ for CFD-ACE.

Most of the gas-phase reactions in the 1995 mechanism are reversible, so it was important to ensure that they were reversible in the CFD-ACE simulations also. The default in CFD-ACE is

irreversible reactions, but reverse rates can either be explicitly supplied or a flag set for them to be obtained from equilibrium (use “BCONST CONST_BY_EQUIL”). Thermochemical and transport data for CFD-ACE is similar in format to that used in CHEMKIN and were easily transferred. Thermochemical data were obtained from quantum chemistry calculations done at SNL in the case of the Si-O-H-C species,⁸ and from standard sources such as the JANAF tables⁹, the CFD-ACE database, or the CHEMKIN Thermodynamic Database¹⁰ for other species.

The most significant issue, however, lay in transferring surface chemistry. CFD-ACE generally treats gas-surface reactions as simple sticking coefficients (i.e. reaction probabilities), although specified rate laws can be hard-wired into customized versions of the code. In contrast, the codes using Surface-CHEMKIN can handle detailed descriptions of wide variety of surface reactions such as coverage-dependent direct or dissociative adsorption of gas-phase species, interconversion reactions between surface species with or without the generation of gas-phase products, and conversion of surface-species to specific “deposited” materials. Although the 1995 mechanism does not use all of these options, it does include what is effectively a coverage-dependent gas-surface reaction, expressed as the presence of multiple surface species where only one reacts with gas-phase species, which could not be simply transferred to CFD-ACE. Rather than work out a rate expression to be inserted in a customized version of CFD-ACE, the sticking coefficients for the initial adsorption reactions in the Surface-CHEMKIN were used in the standard version of CFD-ACE for this work, i.e. the last two surface reactions were dropped. The deposition rates predicted in these simulations represent an upper bound to what would be obtained if the full mechanism could be used, as the other surface species included in the dropped reactions decrease the effective sticking coefficient by blocking surface sites.

Tables 4 and 5 show the chemistry part of the CFD-ACE input file and the input file for thermochemical/transport data for the 1995 mechanism, respectively. Note that the intermediate species formed by gas-phase reactions are simply called INT1 and INT2, although the thermochemical and transport data correspond to the molecules specified in the CHEMKIN mechanism.

Simulations using this mechanism were run for the nominal conditions (500 °C) used in the CVD reactor.³ The deposition rate predicted was 3.5 times higher than observed experimentally. This

Table 4. Chemistry part of CFD-ACE input file for 1995 mechanism

```

MODELS
REACT  GENERAL_RATE  NON_STIFF
RSTEP  1  LHS    1.0 O3  + 1.0 M
RSTEP  1  RHS    1.0 O2  + 1.0 O  + 1.0 M
RSTEP  1  FCONST APF=1.0E10  EF=9058.2
RSTEP  1  BCONST APF=2.03E5  EF=-3255
RSTEP  2  LHS    2.0 O3
RSTEP  2  RHS    3.0 O2
RSTEP  2  FCONST APF=5.0E10  EF=11071.7
RSTEP  2  BCONST APF=5.75E5  EF=46256
RSTEP  3  LHS    1.0 O  + 1.0 TEOS
RSTEP  3  RHS    1.0 INT1 + 1.0 CH3HCO
RSTEP  3  FCONST APF=5.0E13  EF=2516.2
RSTEP  3  BCONST APF=5.88E-2 EF=-567.2
RSTEP  4  LHS    1.0 O3  + 1.0 TEOS
RSTEP  4  RHS    1.0 O2  + 1.0 INT1 + 1.0 CH3HCO
RSTEP  4  FCONST APF=4.0E09  EF=2516.2
RSTEP  4  BCONST CONST_BY_EQUIL
RSTEP  5  LHS    1.0 INT1 + 1.0 M
RSTEP  5  RHS    1.0 INT2 + 1.0 CH3CH2OH + 1.0 M
RSTEP  5  FCONST APF=4.0E09  EF=10064.9
RSTEP  5  BCONST APF=0.0  EF=0.0
CVD_REACTION ON
SURFACE_REACTION FIRST
RSTEP  1  LHS    1.0 INT1
RSTEP  1  RHS    1.0 H2O + 2.0 C2H4 + 1.0 CH3CH2OH + 1.0 OX1
RSTEP  1  CONST APF=0.05  EF=0.0  DEP=OX1  DEN=2240.0
RSTEP  2  LHS    1.0 TEOS
RSTEP  2  RHS    1.0 H2O + 3.0 C2H4 + 1.0 CH3CH2OH + 1.0 OX1
RSTEP  2  CONST APF=4.0E-6 EF=0.0  DEP=OX1  DEN=2240.0
END

```

suggests that either the mass transport was too simplified in the SPIN simulations, and/or that the coverage dependent surface chemistry that got dropped is, in fact, kinetically important. CFD-ACE simulations done at varying substrate temperature gave maximum static-print deposition rates of 18,880 Å/min at 250 °C, 17,600 Å/min at 500 °C, and 14,000 Å/min at 600 °C. This trend qualitatively agrees with the experimental data and SPIN simulations, although the deposition rates are all high.

Figures 1-4 give more detailed results from the CFD-ACE simulations of the WJ tool. Figure 1 shows the mass fractions of the various gas-phase chemical species at the surface as a function of distance from the centerline. Figures 2-4 show the spatial distributions of various gas-phase species from the CFD-ACE simulations. Using the 1995 mechanism, the TEOS is rapidly consumed near the injector to form INT1, which gets transported to the surface and deposits SiO₂ on the wafer. INT2, a non-reactive by-product, forms in the gas-phase and accumulates in parts of the reactor away from the wafer. Ozone (O₃) is also consumed near the injectors, but the highly reactive O atoms formed by this decomposition are themselves consumed by reaction with

Table 5. Thermochemical and transport input file for CFD-ACE

O3	O	3	100.0	5000.0	48.0
0.54665239E 01	0.17326031E-02	-0.72204889E-06	0.13721660E-09	-0.96233828E-14	
0.15214096E 05	-0.34712616E 01	0.24660617E 01	0.91703209E-02	-0.49698480E-05	
-0.20634230E-08	0.20015595E-11	0.16059556E 05	0.12172130E+02		
1.405E-6	111.50	180.0	4.10		
TEOS	O	4SI 1C 8H 20	100.0	5000.0	208.0
0.14384550E+02	0.91940556E-01	-0.48408362E-04	0.12244826E-07	-0.12086997E-11	
-0.16779748E+06	-0.26402920E+02	0.36650096E+01	0.11162005E+00	-0.42142822E-04	
-0.16446561E-07	0.12257199E-10	-0.16452653E+06	0.31030103E+02		
1.405E-6	111.50	522.7	7.03		
INT1	O	4SI 1C 6H 16	100.0	5000.0	180.0
0.30722271E+02	0.30770605E-01	-0.25774402E-05	-0.30498899E-08	0.66850084E-12	
-0.17340573E+06	-0.11836710E+03	0.89422655E+01	0.70058122E-01	-0.53697897E-06	
-0.37873331E-07	0.15943972E-10	-0.16629886E+06	-0.43492889E+00		
1.405E-6	111.50	522.7	7.03		
INT2	O	7SI 2C 12H 30	100.0	5000.0	342.0
2.37118816E+01	1.38595819E-01	-7.21792312E-05	1.81146351E-08	-1.77790129E-12	
-2.97149250E+05	-6.43604507E+01	1.70925987E+0	1.97589725E-01	-1.16528972E-04	
1.78428774E-08	5.85231559E-12	-2.91318375E5	4.89922791E+01		
1.405E-6	111.50	522.7	8.0		
CH3HCO	O	1C 2H 3	100.0	5000.0	44.0
0.05868650E+02	0.01079424E+00	-0.03645530E-04	0.05412912E-08	-0.02896844E-12	
-0.02264569E+06	-0.06012946E+02	0.02505695E+02	0.01336991E+00	0.04671953E-04	
-0.01128140E-06	0.04263566E-10	-0.02124589E+06	0.01335089E+03		
1.405E-6	111.50	436.0	3.97		
C2H5OH	O	1C 2H 6	100.0	5000.0	46.0
0.64007540E 01	0.14915377E-01	-0.49970376E-05	0.73528339E-09	-0.38892277E-13	
-0.25361430E 05	-0.10026032E 02	0.28873615E 01	0.15707601E-01	0.76206034E-05	
-0.13889426E-07	0.46893826E-11	-0.23739500E 05	0.10835417E+02		
1.405E-6	111.50	424.7	4.16		
OX1	O	2SI 1	100.0	5000.0	60.0
0.58620395E 01	0.17719784E-02	-0.75194194E-06	0.14180584E-09	-0.98856417E-14	
-0.38767816E 05	-0.68603501E 01	0.32628058E 01	0.85016584E-02	-0.57388144E-05	
0.12896573E-10	0.97544976E-12	-0.38035971E 05	0.66549123E 01		
1.405E-6	111.50	2954.0	3.71		
OH	O	1H 1	100.0	5000.0	17.0
2.88273048E+00	1.01397431E-03	-2.27687707E-07	2.17468370E-11	-5.12630534E-16	
3.88688794E+03	5.59571219E+00	3.63726592E+00	1.85091049E-04	-1.67616463E-06	
2.38720266E-09	-8.43144185E-13	3.60678174E+03	1.35886049E+00		
1.405E-6	111.50	80.0	2.75		
H	H	1	100.0	5000.0	1.0
2.50000000E+00	0.00000000E+00	0.00000000E+00	0.00000000E+00	0.00000000E+00	
2.54716270E+04	-4.60117608E-01	2.50000000E+00	0.00000000E+00	0.00000000E+00	
0.00000000E+00	0.00000000E+00	2.54716270E+04	-4.60117638E-01		
6.89E-07	96.69	145.0	2.05		

TEOS to form INT1. They do, however, build up in regions away from the wafer, which is unphysical and is probably caused by the lack of an O atom recombination reaction in the mechanism. Water vapor (H₂O) and ethylene (C₂H₄) are produced by surface reactions and have their highest concentrations near the wafer, as expected. The spatial distributions of acetaldehyde (CH₃HCO) and ethanol (C₂H₅OH) reflect the fact that they are formed in the gas-phase along with INT1 and INT2, respectively, although they are also formed by surface reactions.

To test the sensitivity of these simulations to the surface chemistry, the sticking coefficient for INT1 was varied. The deposition rate did not change when the sticking coefficient was increased from 0.05 to 1.0, which suggests that gas-phase reactions or mass transport are kinetically important. In contrast, as the sticking coefficient was decreased, a decrease in deposition rate was observed. This suggests that the kinetic bottleneck is being shifted to the surface reactions, and that accounting for the coverage dependence may be important. As shown in Fig. 5, decreasing this sticking coefficient from 0.05 to 0.001 gave a maximum deposition rate of 10,000 Å/min at 500 °C, while further decreasing it to 0.0001 gave a deposition rate slightly over 2000 Å/min. Decreasing the sticking coefficient by a factor of 50 has about the same effect as blocking 98% of the surface sites, which is plausible at these surface temperatures. Although if the surface has a high coverage of ethoxy or other “blocking” groups, reactions of O atoms or ozone that “clean” the surface probably need to be considered. But the observed effect of changing the sticking coefficient suggests a reasonable approach for tuning this mechanism, if desired.

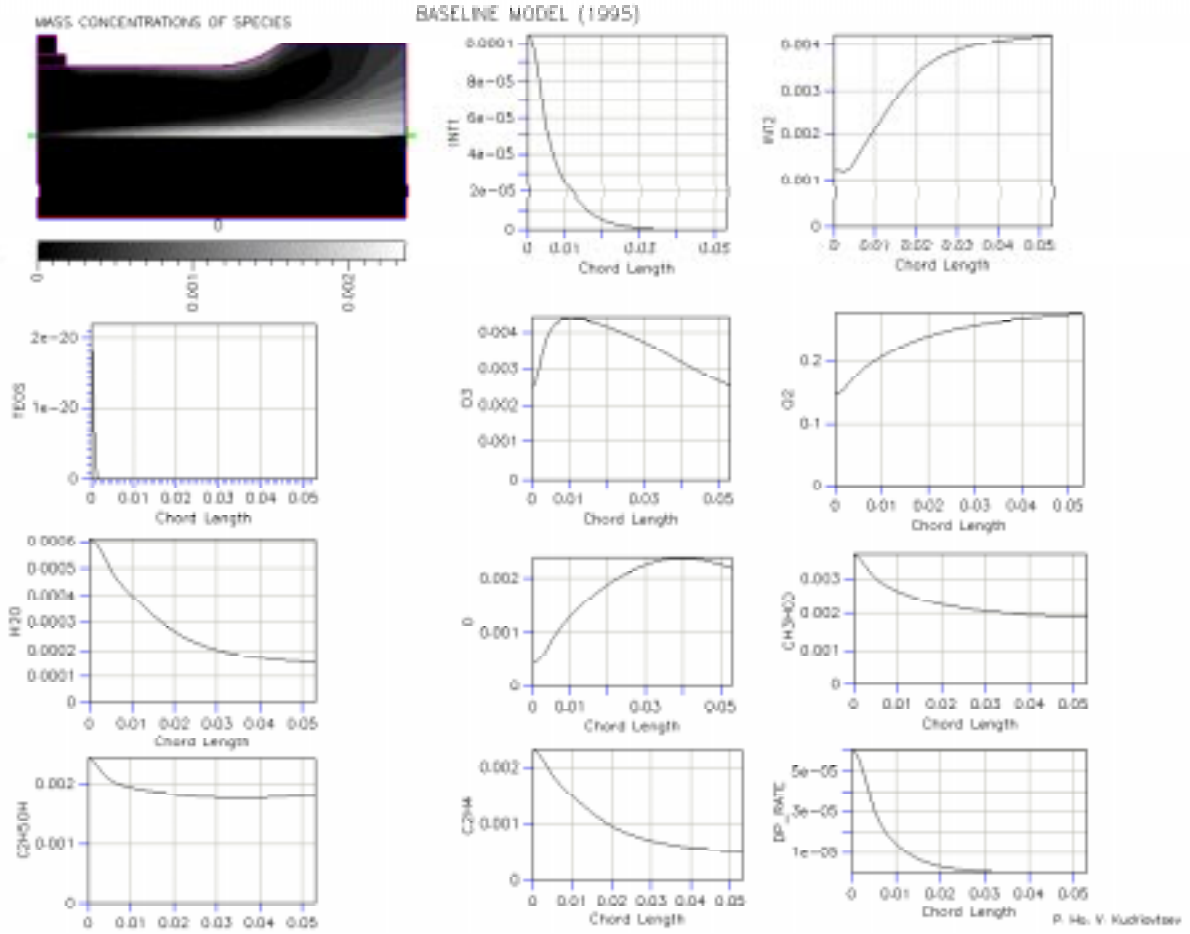


Figure 1. Mass fractions of various chemical species at the surface as a function of distance from wafer centerline, 1995 mechanism.

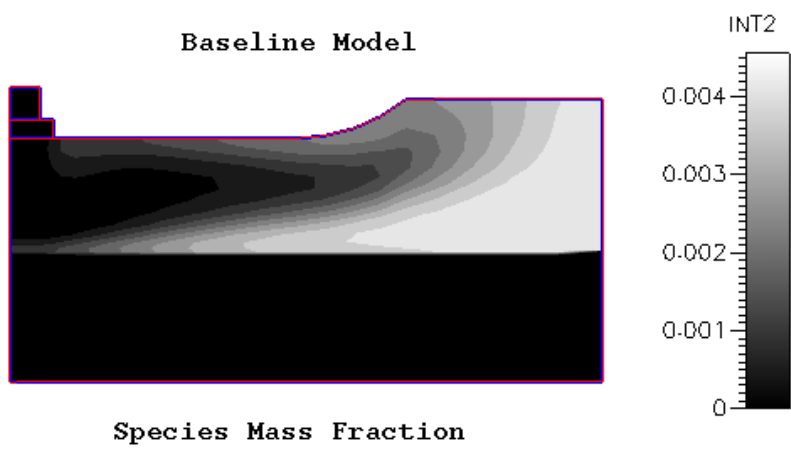
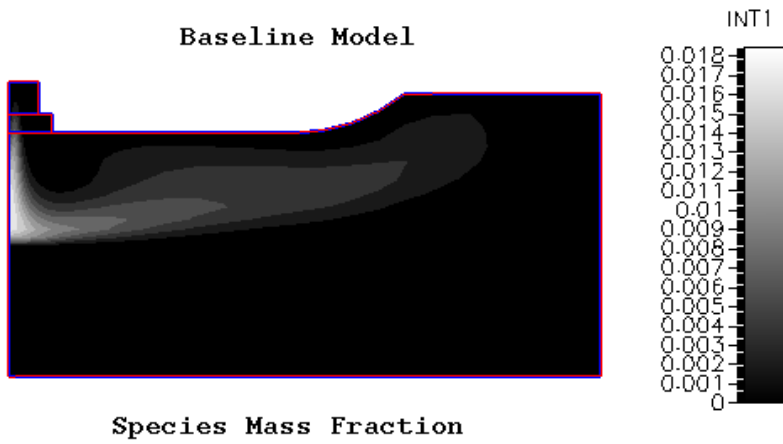
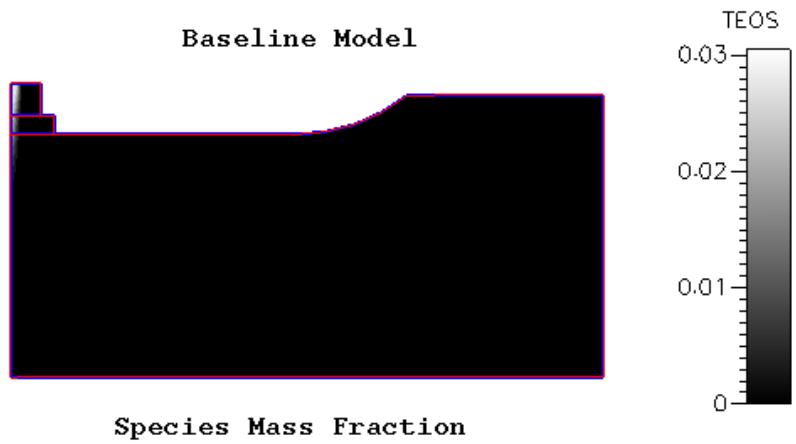


Figure 2. Spatial distributions of TEOS, INT1 and INT2, 1995 mechanism.

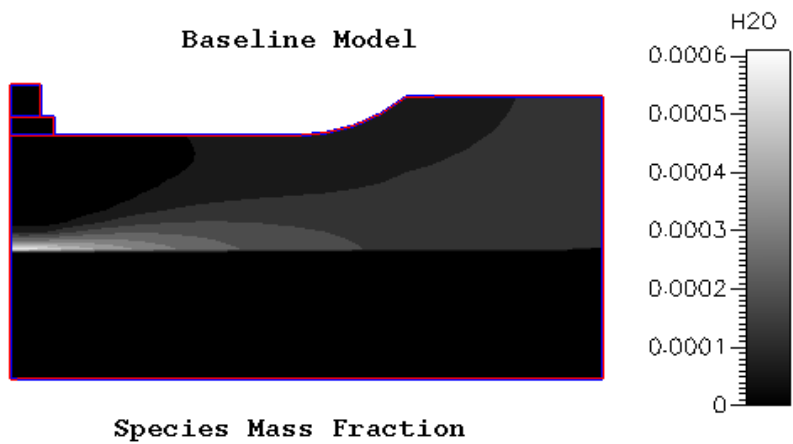
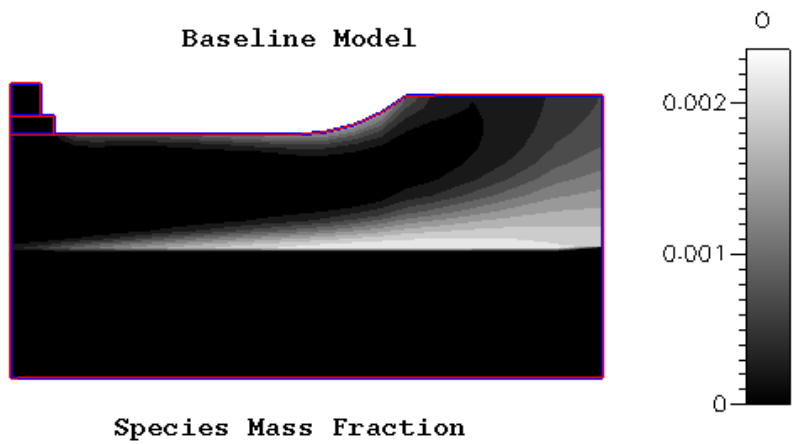
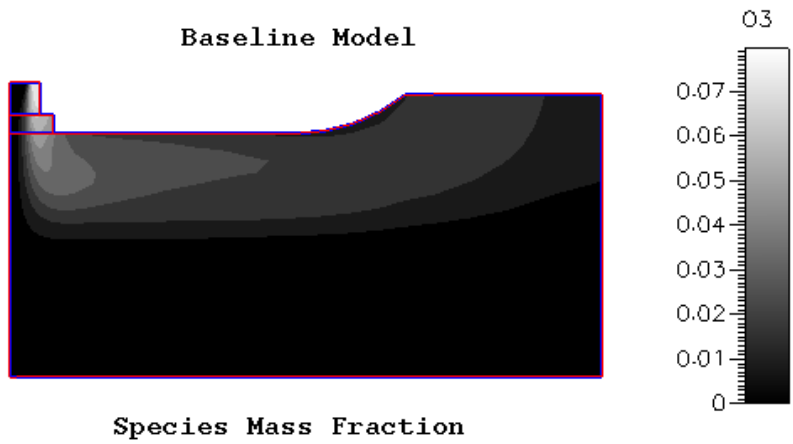


Figure 3. Spatial distributions of O₃, O and H₂O, 1995 mechanism.

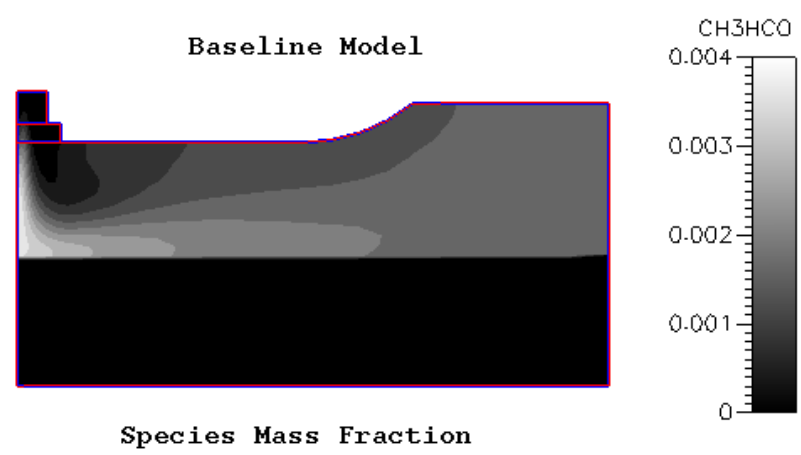
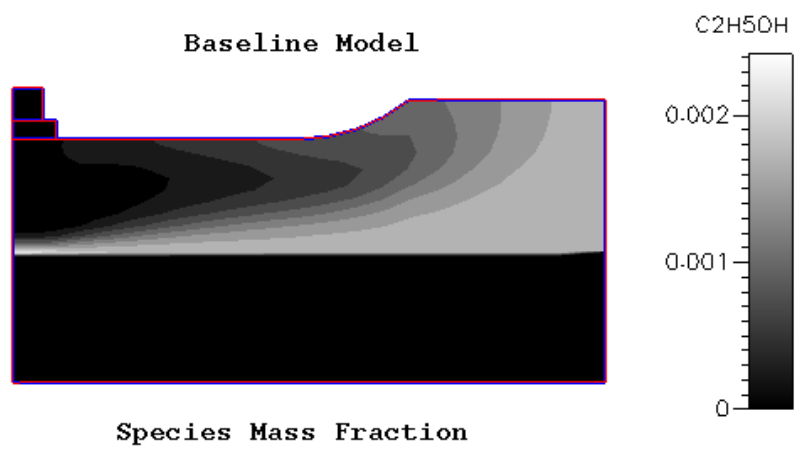
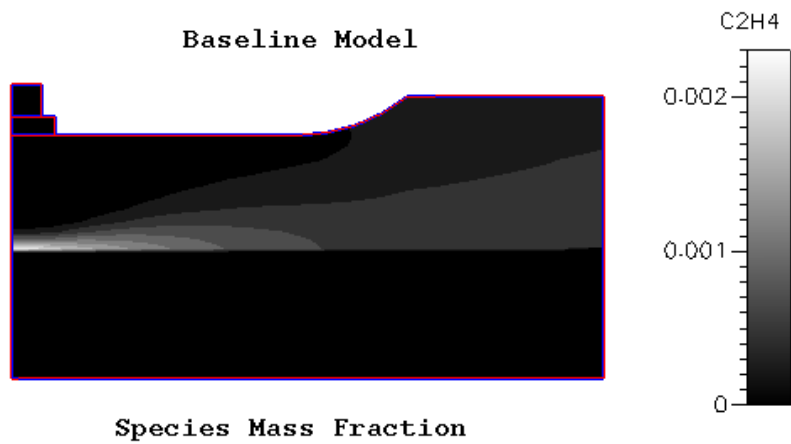


Figure 4. Spatial distributions of C₂H₄, C₂H₅OH and CH₃CHO, 1995 mechanism.

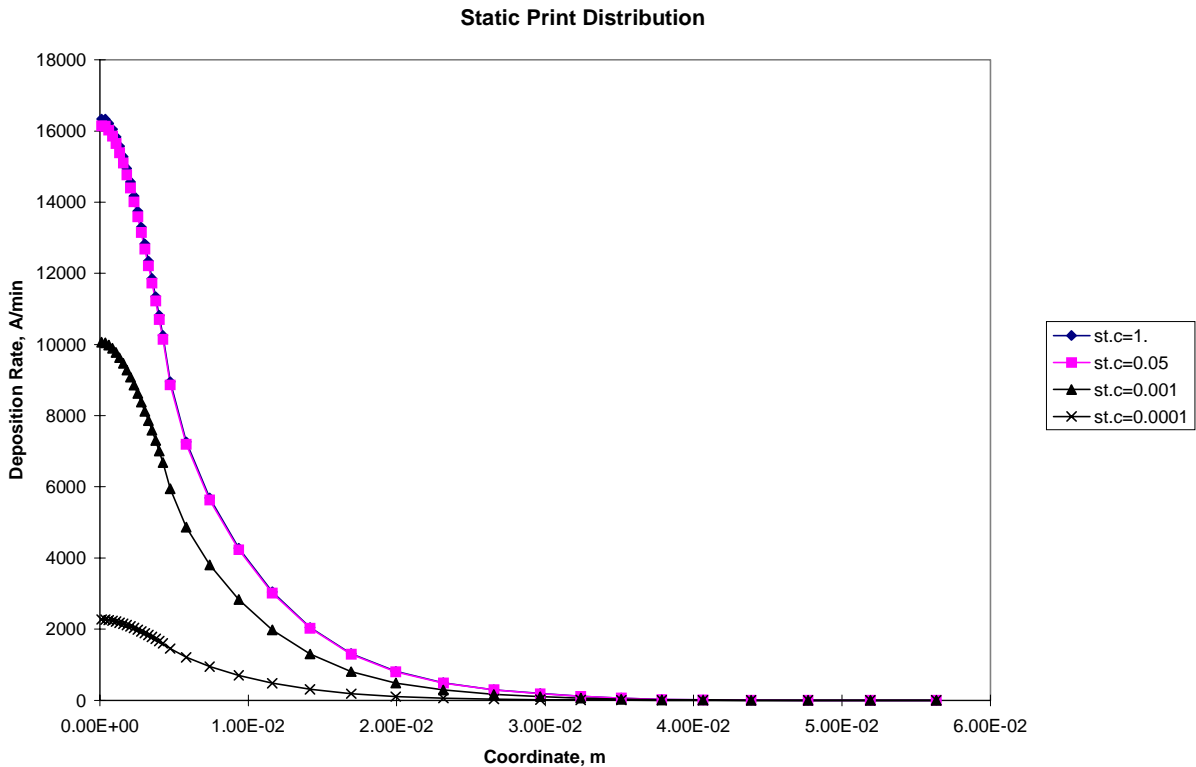


Figure 5. Two dimensional simulations of static prints using different values of the INT1 sticking coefficient.

IV. New mechanism development

Development of a new reaction mechanism for the TEOS/O₃ system was also started, based on the knowledge currently available. The first version of this new mechanism still used “lumped” reactions, and included the following. 1) The ozone decomposition mechanism of Benson and Axworthy,¹¹ which is comprised of the reactions $O_3 + M \leftrightarrow O + O_2 + M$ (where M stands for all colliding molecules) and $O + O_3 \leftrightarrow 2 O_2$. 2) The third-body stabilized recombination of O atoms $2 O + M \leftrightarrow O_2 + M$, taken from the work in the literature by Tsang and Hampson.¹² This reaction is needed to prevent the unphysical build-up of O atoms in the gas-phase that was observed in the simulations using the 1995 mechanism. 3) The $O + TEOS \leftrightarrow INT1 + CH_3CHO$ reaction, using an experimentally-measured rate constant recently reported by Buchta, et al.,¹³

rather than the previously used estimates. Note that INT1, a placeholder for what is probably a variety of species, is still being treated as if it were $\text{Si}(\text{OC}_2\text{H}_5)_3\text{OH}$. 4) The reaction of INT1 with the surface, with a sticking coefficient of 1.0 for maximum effect.

Table 6 gives the CFD-ACE input file for this mechanism (the thermochemical and transport data in Table 5 were again used). Some preliminary simulations were done, and at the nominal conditions, this mechanism appears to give deposition rates that are low by roughly a factor of ten. Altering the sticking coefficient for INT1 had only a small effect on the deposition rate. This suggests that the gas-phase reactions that form the intermediate, rather than surface reactions of the intermediate, were rate-limiting in this case. Mass transport effects, however, also appear to be very important.

Figures 6-8 give more detailed results from these simulations. Figure 6 shows the mass fractions of the various gas-phase chemical species at the surface as a function of distance from the centerline. Figures 7 and 8 show the spatial distributions of various gas-phase species from the CFD-ACE simulations. For this reaction mechanism, the TEOS and O_3 are consumed to a much lesser degree, as would be expected with the much lower deposition rates, and reasonable amounts of these species are present in the reactor. INT1 accumulates in parts of the reactor away from the surface. This probably results from the fact that there are no gas-phase loss terms

Table 6. Chemistry part of CFD-ACE input file for new mechanism	
RSTEP 1	LHS 1.0 O3 + M
RSTEP 1	RHS 1.0 O2 + 1.0 O + M
RSTEP 1	FCONS APF=4.61E12 EF=12085 AF_O3=1
RSTEP 1	BCONS APF=6.00E+7 EF=-302. AF_O2=1 AF_O=1
RSTEP 1	3BFAC C3_O3=1. C3_O2=.44 C3_N2=.41
RSTEP 2	LHS 1.0 O3 + 1.0 O
RSTEP 2	RHS 2.0 O2
RSTEP 2	FCONS APF=2.96E10 EF=3021. AF_O3=1 AF_O=1
RSTEP 2	BCONS APF=0. EF=0.
RSTEP 3	LHS 1.0 O + 1.0 O + M
RSTEP 3	RHS 1.0 O2 + M
RSTEP 3	FCONS APF=1.89E7 EF=-900.
RSTEP 3	BCONS APF=0. EF=0.
RSTEP 4	LHS 1.0 O + 1.0 TEOS
RSTEP 4	RHS 1.0 INT1 + 1.0 CH3HCO
RSTEP 4	FCONST APF=2.7E9 EF=1320.62
RSTEP 4	BCONST APF=0 EF=0
CVD_REACTION ON	
SURFACE_REACTION FIRST	
RSTEP 1	LHS 1.0 INT1
RSTEP 1	RHS 1.0 H2O + 2.0 C2H4 + 1.0 C2H5OH + 1.0 OX1
RSTEP 1	CONST APF=1.0 EF=0. DEP=OX1 DEN=2240.0
END	

for this species; the reaction forming INT1 was made irreversible in this case. In contrast with the results in Fig. 3, the O atoms now are quickly consumed, either by reaction with TEOS or recombination, which is more reasonable physically. CH_3CHO shows a maximum near the surface, which suggests that the $\text{O} + \text{TEOS}$ reaction is occurring near the surface in this case. CH_3CHO is formed by the same reaction that forms INT1, and, as expected, shows a similar spatial distribution, although there are differences. C_2H_4 is formed only by the surface reaction of INT1, and, as expected, its mass fraction is highest near the surface and decreases with distance above it.

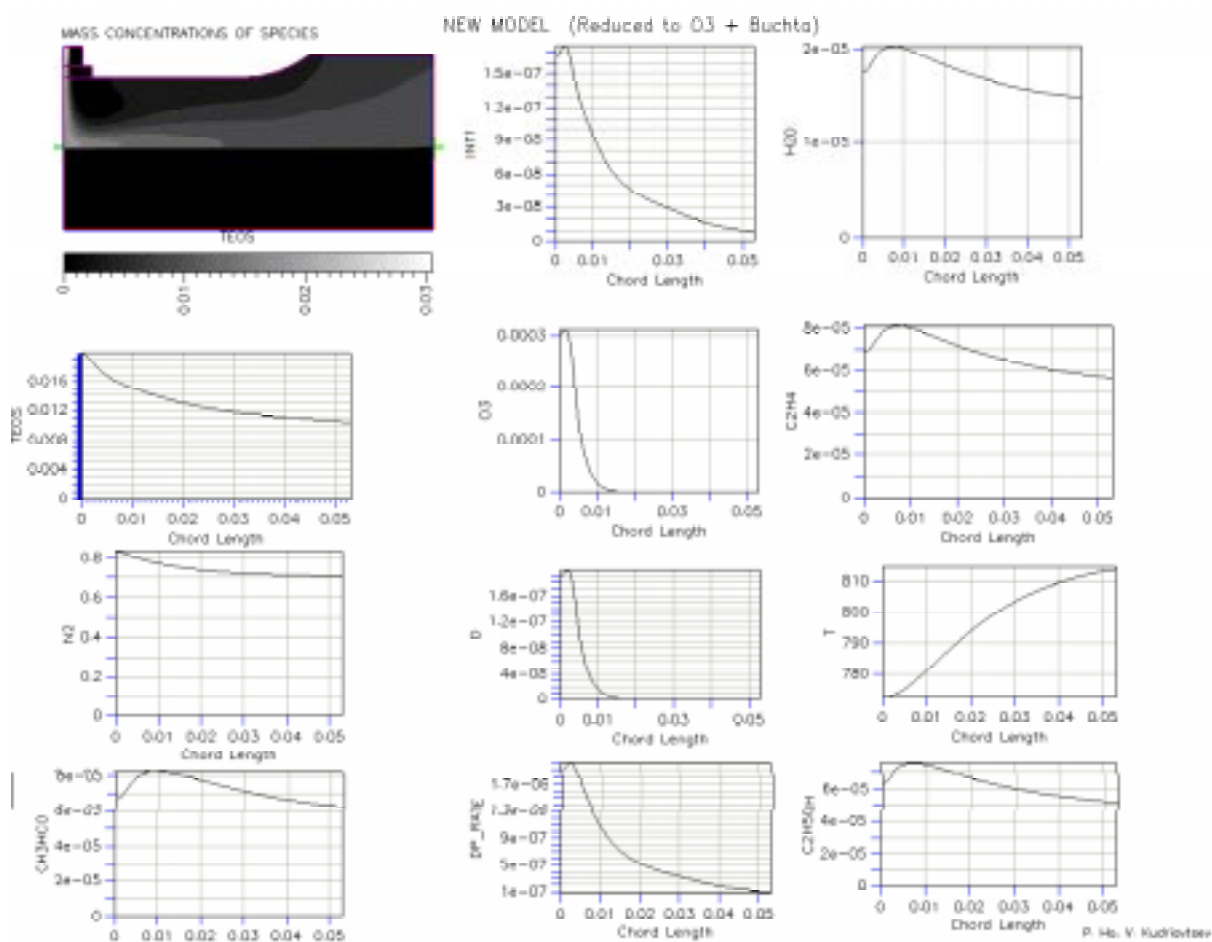


Figure 6. Mass fractions of various chemical species at the surface as a function of distance from wafer centerline, new mechanism.

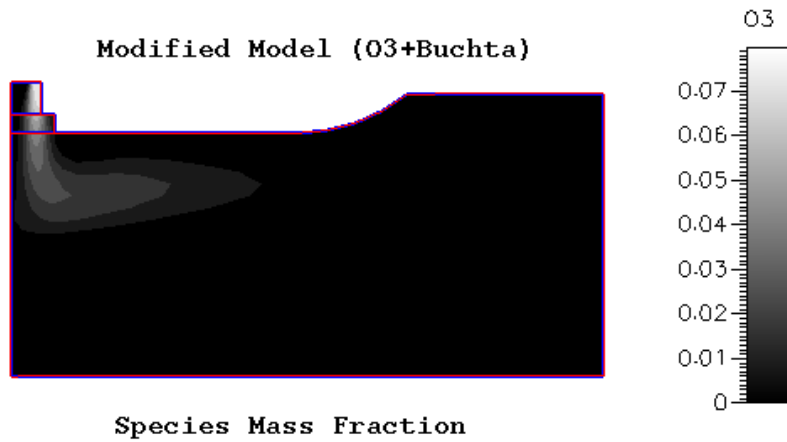
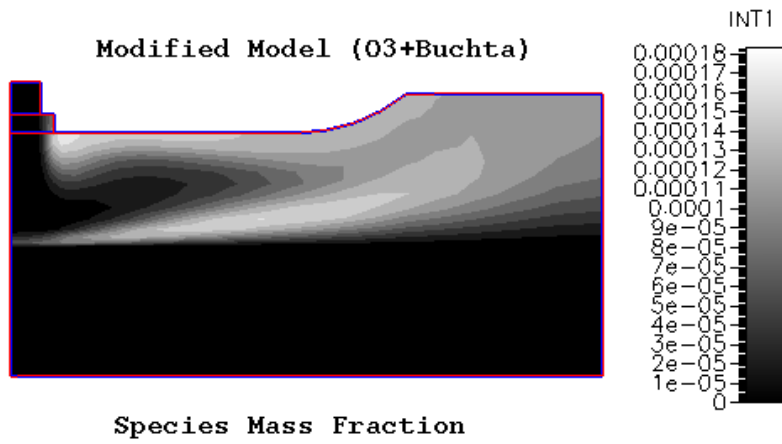
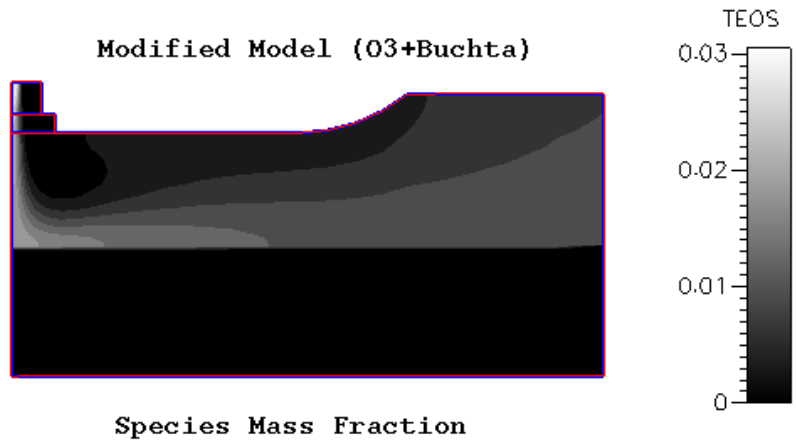


Figure 7. Spatial distributions of TEOS, INT1 and O₃, new mechanism.

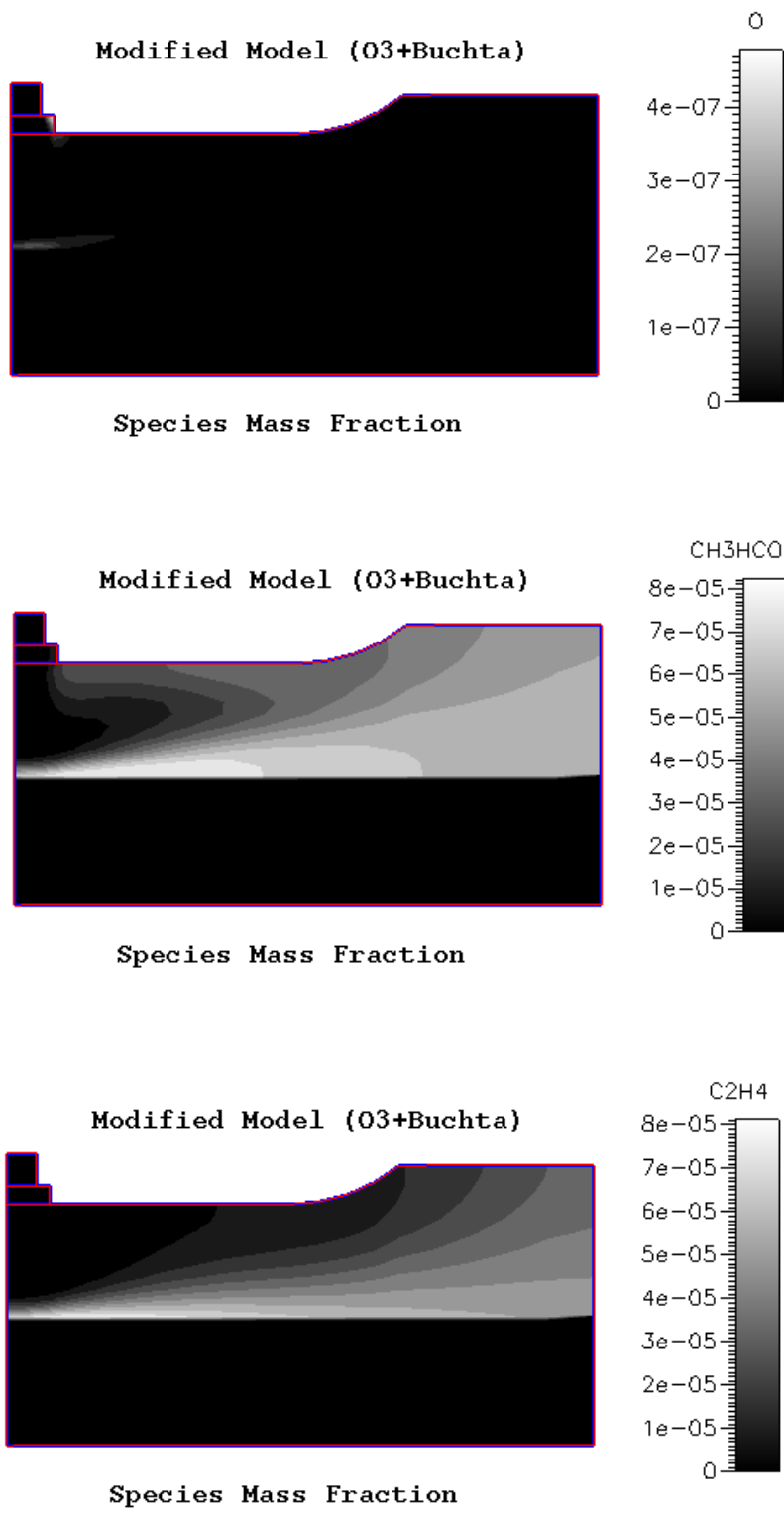


Figure 8. Spatial distributions of O, CH₃CHO and C₂H₄, new mechanism.

However, the approach taken here still represents a substantial oversimplification of the chemistry occurring in the TEOS/O₃ system. The elementary reactions that really occur are far more complicated. For example, it is certain that the O + TEOS reaction does not directly produce Si(OC₂H₅)₃OH + CH₃CHO, although it has been written that way in the mechanisms for convenience. Instead, the O atom probably abstracts a H atom from one of the ethoxy groups on TEOS, forming OH + C₂H₄OSi(OC₂H₅)₃. The OH radical could then abstract an H atom from another TEOS molecule forming H₂O + C₂H₄OSi(OC₂H₅)₃, or react with an O atom, O₃ molecule, or the surface. C₂H₄OSi(OC₂H₅)₃ could eliminate a C₂H₄ group to form a OSi(OC₂H₅)₃ radical, undergo other internal rearrangements to eliminate some other species, react with an O atom, O₃ molecule, the surface, or some other gas-phase species to start polymerizing. A radical chain of some sort is also likely, as are condensation reaction of 2 Si(OC₂H₅)₃OH molecules or Si(OC₂H₅)₃OH with TEOS to form Si(OC₂H₅)₃OSi(OC₂H₅)₃. This is a somewhat more realistic way of depleting the intermediate in the gas phase than secondary elimination reaction contained in the 1995 mechanism. It also represents a possible first step in the formation of TEOS “polymers” on the way to gas-phase particle nucleation.

The reasonableness of such reactions can be evaluated using thermochemical data that became available a few years ago,⁸ plus estimates derived using group-additivity concepts. Table 7 lists a few example reactions of possible interest for TEOS/O₃ CVD along with heats of reaction. These data show that, for example, the elementary reaction proposed above, C₂H₄OSi(OC₂H₅)₃ → C₂H₄ + OSi(OC₂H₅)₃, is endothermic by 38 kcal/mole. This endothermicity makes the reaction less likely to occur, although it would be counteracted by entropy considerations, especially at elevated temperatures. In contrast, the reaction C₂H₄OSi(OC₂H₅)₃ + O₃ → O₂ + CH₃CHO + OSi(OC₂H₅)₃ is exothermic, but is not an elementary reaction. The reaction between C₂H₄OSi(OC₂H₅)₃ and O₃ probably forms a species like OC₂H₄OSi(OC₂H₅)₃ for which a heat of formation is not available at this time.

The thermochemistry is also the first step toward obtaining rate parameters, although activation energies often differ significantly from heats of reaction. The first reaction in Table 7, the elimination of ethylene from TEOS, illustrates this point. This reaction, which is believed to be important in TEOS CVD at higher temperatures, is endothermic by only 10 kcal/mole, but has a

Table 7: Some reactions relevant to TEOS/O ₃ CVD	$\Delta H^{\circ}\text{rxn}$ (kcal/mole)
$\text{Si}(\text{OC}_2\text{H}_5)_4 \rightarrow \text{Si}(\text{OC}_2\text{H}_5)_3\text{OH} + \text{C}_2\text{H}_4$	10.5
$\text{Si}(\text{OC}_2\text{H}_5)_4 + \text{O} \rightarrow \text{OH} + \text{C}_2\text{H}_4 + \text{OSi}(\text{OC}_2\text{H}_5)_3$	34.5
$\text{Si}(\text{OC}_2\text{H}_5)_4 + \text{O} \rightarrow \text{OH} + \text{CH}_3\text{CHO} + \text{Si}(\text{OC}_2\text{H}_5)_3$	42.9
$\text{Si}(\text{OC}_2\text{H}_5)_4 + \text{O} \rightarrow \text{Si}(\text{OC}_2\text{H}_5)_3\text{OH} + \text{CH}_3\text{CHO}$	-99.8
$\text{Si}(\text{OC}_2\text{H}_5)_4 + \text{O} \rightarrow \text{OH} + \text{C}_2\text{H}_4\text{OSi}(\text{OC}_2\text{H}_5)_3$	-3.9
$\text{Si}(\text{OC}_2\text{H}_5)_4 + \text{O}_3 \rightarrow \text{OH} + \text{C}_2\text{H}_4\text{OSi}(\text{OC}_2\text{H}_5)_3 + \text{O}_2$	21.0
$\text{Si}(\text{OC}_2\text{H}_5)_4 + \text{OH} \rightarrow \text{H}_2\text{O} + \text{C}_2\text{H}_4\text{OSi}(\text{OC}_2\text{H}_5)_3$	-21.3
$\text{C}_2\text{H}_4\text{OSi}(\text{OC}_2\text{H}_5)_3 \rightarrow \text{C}_2\text{H}_4 + \text{OSi}(\text{OC}_2\text{H}_5)_3$	38.4
$\text{C}_2\text{H}_4\text{OSi}(\text{OC}_2\text{H}_5)_3 \rightarrow \text{CH}_3\text{CHO} + \text{Si}(\text{OC}_2\text{H}_5)_3$	46.8
$\text{C}_2\text{H}_4\text{OSi}(\text{OC}_2\text{H}_5)_3 + \text{O}_3 \rightarrow \text{O}_2 + \text{CH}_3\text{CHO} + \text{OSi}(\text{OC}_2\text{H}_5)_3$	-47.0
$\text{C}_2\text{H}_4\text{OSi}(\text{OC}_2\text{H}_5)_3 + \text{O}_2 \rightarrow \text{CH}_3\text{COOH} + \text{OSi}(\text{OC}_2\text{H}_5)_3$	-77.7
$\text{OSi}(\text{OC}_2\text{H}_5)_3 + \text{Si}(\text{OC}_2\text{H}_5)_3 \rightarrow \text{O}(\text{Si}(\text{OC}_2\text{H}_5)_3)_2$	-130.9
$\text{OSi}(\text{OC}_2\text{H}_5)_3 + \text{Si}(\text{OC}_2\text{H}_5)_4 \rightarrow \text{HOSi}(\text{OC}_2\text{H}_5)_3 + \text{C}_2\text{H}_4\text{OSi}(\text{OC}_2\text{H}_5)_3$	-27.9
$2 \text{Si}(\text{OC}_2\text{H}_5)_3\text{OH} \rightarrow \text{H}_2\text{O} + \text{O}(\text{Si}(\text{OC}_2\text{H}_5)_3)_2$	18.4
$\text{Si}(\text{OC}_2\text{H}_5)_3\text{OH} + \text{Si}(\text{OC}_2\text{H}_5)_4 \rightarrow \text{O}(\text{Si}(\text{OC}_2\text{H}_5)_3)_2 + \text{C}_2\text{H}_5\text{OH}$	17.3
$\text{Si}(\text{OC}_2\text{H}_5)_3\text{OH} \rightarrow \text{O}=\text{Si}(\text{OC}_2\text{H}_5)_2 + \text{C}_2\text{H}_5\text{OH}$	69.7
$\text{O} + \text{H} \rightarrow \text{OH}$	-102.0
$\text{H}_2\text{O} \rightarrow \text{H} + \text{OH}$	119.4
$\text{OH} + \text{O}_2 \rightarrow \text{HO}_2 + \text{O}$	53.5
$\text{OH} + \text{O}_3 \rightarrow \text{HO}_2 + \text{O}_2$	-40.4
$\text{HO}_2 \rightarrow \text{H} + \text{O}_2$	48.5
$\text{O}_2 \rightarrow 2 \text{O}$	118.8
$2 \text{O}_3 \rightarrow 3 \text{O}_2$	-69.0
$\text{O}_3 \rightarrow \text{O} + \text{O}_2$	24.9
$\text{O} + \text{O}_3 \rightarrow 2 \text{O}_2$	-93.9

much higher activation energy of ~60-70 kcal/mole. Although Table 7 is a very incomplete list and many of these reactions are not elementary, it illustrates the process of writing down possible reactions and then evaluating their likeliness using thermochemistry. A more complete study of this sort would be an important part of developing a more fundamentally-based mechanism.

An optimal mechanism would also include a variety of surface species and reactions. Although there is generally much less information available in the literature to draw on in terms of measured or estimated thermochemical or kinetic data, it is believed that, for many CVD systems, surface reactions are more important than gas-phase processes. A description of how the gas/surface reactions depend on the coverage of the surface with various groups is often necessary to describe how deposition rates vary over widely ranging temperatures and input gas compositions. A detailed description of surface reactions is often crucial to modeling the effects

of dopant species on deposition rates. In addition, a detailed treatment of surface reactions, in terms of describing the competition between the removal of ethoxy groups from the surface vs. “burying them” under the next layer of oxide, could allow the simulation of how film properties, specifically carbon incorporation in the film, depend on reactor conditions.

Although not explicitly discussed here, there are a number of studies in the literature that should assist the mechanism development process. In addition to mechanistic studies of TEOS reactions with O atoms and ozone, these include chemical kinetics studies of related reactions (for example, hydrocarbon combustion), parametric studies of TEOS, plasma TEOS and/or TEOS/O₃ CVD under widely varying conditions, and surface-science studies of elementary reactions on SiO₂ surfaces.

V. Summary

A reaction mechanism for TEOS/O₃ CVD that was originally developed and tuned to WJ deposition rate data in 1995 at Sandia was implemented in reactor simulations at WJ. Simulations done for nominal reactor conditions gave predicted deposition rates that were roughly $\times 3.5$ higher than experiment. This discrepancy suggests that either the SPIN simulations used to develop the mechanism contained a too-simple description of the heat and mass transport in the system, or that the coverage-dependent surface reactions that were dropped because of limitations in the modeling software are important to this chemistry. The fact that decreasing the sticking coefficient for the reaction of the gas-phase intermediate with the surface improved the agreement between the model predictions and the experiment supports the latter contention, but this needs to be tested over a wider range of conditions.

In the immediate future, work should be targeted at developing a more fundamentals-based reaction mechanism, although it will still need to be tuned to reactor data. This process was started as part of this project, but the initial mechanism gave deposition rates that were too low, suggesting the need for a more complete treatment of the chemistry. There is a reasonable amount of independent information available to help in developing a such a mechanism for TEOS/O₃ CVD.

In the short term, the description of the surface reactions in the mechanism is limited by the inability of the CFD software to handle multiple surface species and surface reactions with arbitrarily complex coverage dependencies. Such capabilities are crucial to modeling how film properties such as carbon incorporation in the film depend on reactor conditions, or the effects of dopant species on deposition rates. Also, there will always be tradeoffs between the complexity of the chemical mechanisms used and the computational speed of the simulations. During development of a complex reaction mechanism, there usually are advantages to using a simplified simulation of the reactor that runs faster.

Acknowledgments

We thank John Boland for his support of this project. We acknowledge the contributions of Dr. Simin Mokhtari of Watkins-Johnson to the work done in 1995. We thank Dr. Ning Zhou and Mr. Mark Rist from CFD Research Corporation for their help in developing the CFD models used in this work. This work was funded by Watkins-Johnson Company under a Technical Assistance Agreement with Sandia National Laboratories. Sandia is a multiprogram laboratory operated by Sandia Corporation, a Lockheed Martin Company, for the United States Department of Energy under Contract DE-AC04-94AL85000.

References

- ¹ See for example, I. A. Shareef, G. W. Rubloff, and W. N. Gill, *J. Vac. Sci Tech.*, **B14**, 1 (1996), E. J. Kim and W. N. Gill, *J. Cryst. Growth*, **140**, 308, 315 (1994), *J. Electrochem. Soc.*, **141**, 3462 (1994).
- ² D. M. Dobkin, S. Mokhtari, M. Schmidt, A. Pant, L. Robinson, and A. Sherman, *J. Electrochem. Soc.*, **142**, 2332 (1995).
- ³ N. Zhou, A. Krishnan, V. Kudriavtsev, and Y. Brichko, Proceedings of the Fifth International Conference on Advanced Thermal Processing of Semiconductors, New Orleans, Sept. 1997.
- ⁴ M. E. Coltrin, R. J. Kee, G. H. Evans, E. Meeks, F. M. Rupley, and J. F. Grcar, "SPIN (Version 3.83): A Fortran Program for Modeling One-Dimensional Rotating-Disk/Stagnation-Flow Chemical Vapor Deposition Reactors", Sandia National Laboratories Report No SAND91-8003, August 1991.

- ⁵ R. J. Kee, F. M. Rupley, E. Meeks, and J. A. Miller, “CHEMKIN-III: A Fortran Chemical Kinetics Package for the Analysis of Gas-phase Chemical and Plasma Kinetics”, Sandia National Laboratories Report No SAND96-8216, May 1996.
- ⁶ M.E. Coltrin, R. J. Kee, F. M. Rupley, and E. Meeks, “Surface CHEMKIN-III: A Fortran Package for Analyzing Heterogeneous Chemical Kinetics at a Solid-surface – Gas-phase Interface”, Sandia National Laboratories Report No SAND96-8217, May 1996.
- ⁷ Available from CFD Research Corporation, 215 Wynn Drive, Huntsville, Alabama, 35805, www.cfdrc.com.
- ⁸ P. Ho and C. F. Melius, *J. Phys. Chem.*, **99**, 2166 (1995), and supplementary material.
- ⁹ M. W. Chase, Jr., C. A. Davies, J. R. Downey, Jr., D. J. Frurip, R. A. McDonald, and A. N. Syverud, “JANAF Thermochemical Tables, Third Edition”, *J. Phys. Chem. Ref. Data*, **14**, Supplement No. 1, (1985).
- ¹⁰ R. J. Kee, R. M. Rupley, J. A. Miller, “The CHEMKIN Thermodynamic Data Base”, Sandia National Laboratories Report No SAND87-8215B, March 1990.
- ¹¹ S. W. Benson and A. E. Axworthy, Jr., *J. Chem. Phys.*, **26**, 1718 (1957).
- ¹² W. Tsang and R. F. Hampson, *J. Phys. Chem. Ref. Data*, **15**, 1087 (1986).
- ¹³ C. Buchta, H. Gg. Wagner and W. Wittchow, *Z. Phys. Chem.*, **190**, 167 (1995)

Initial Distribution:
Unlimited Release

- 2 Dr. Avishay Katz
Chief Technology Officer
Watkins-Johnson Company
440 Kings Village Road, Scotts Valley, CA 95066

- 2 Mark Danna
VP of Engineering
Watkins-Johnson Company
440 Kings Village Road, Scotts Valley, CA 95066

- 2 Jim Bondur
VP of Plasma Engineering
Watkins-Johnson Company
440 Kings Village Road, Scotts Valley, CA 95066

- 2 Sattar Al-Lami
Manager, Process Integration
Watkins-Johnson Company
440 Kings Village Road, Scotts Valley, CA 95066

- 1 Dr. Simin Mokhtari
Senior Member of the Technical Staff
Watkins-Johnson Company
440 Kings Village Road, Scotts Valley, CA 95066

- 3 John Boland
Manager, Core Engineering
Watkins-Johnson Company
440 Kings Village Road, Scotts Valley, CA 95066

- 40 Dr. Vladimir Kudriavtsev
Senior Member of the Technical Staff
Watkins-Johnson Company
440 Kings Village Road, Scotts Valley, CA 95066

- 5 Neil Fernandes
Manager, Marketing
Watkins-Johnson Company
440 Kings Village Road, Scotts Valley, CA 95066

- 1 Bruce Mayer, Staff Engineer
Watkins-Johnson Company
440 Kings Village Road, Scotts Valley, CA 95066
- 2 Dr. Anantha Krishnan
VP Research
CFD Research Corporation
Cummings Research Park
215 Wynn Drive
Huntsville, AL 35805
- 1 Dr. Ning Zhou
Research Engineer
CFD Research Corporation
Cummings Research Park
215 Wynn Drive
Huntsville, AL 35805
- 1 Dr. Fritz Owens
Manager, Consulting
CFD Research Corporation
Cummings Research Park
215 Wynn Drive
Huntsville, AL 35805
- 1 Prof. W. N. Gill
Rensselaer Polytechnic Institute
Department of Chemical Engineering,
Troy, NY 12180-3590
- 1 Dr. Daniel M. Dobkin
Enigmatics
505 West Olive Ave. #425
Sunnyvale, CA 94086
- 1 Prof. John E. Crowell
Department of Chemistry,
University of California, San Diego
La Jolla, CA 92093-0314
- 1 Dr. Alex Lubnin
656 Southampton Court
Copley, OH 44321

MS

15	0601	P. Ho, 1126
1	0601	J. Y. Tsao, 1126
5	0827	J. Johannes, 9114
1	0827	J. E. Brockman, 9114
1	0827	R. O. Griffith, 9114
1	0841	P. J. Hommert, 9100
1	1077	L. Cecchi, 1326
1	1380	M. Sanders, 4212
1	1427	S. T. Picraux, 1100
1	9018	Central Technical Files, 8940-2
5	0899	Technical Library, 4916
2	0619	Review & Approval Desk, 12690 For DOE/OSTI